IRON CHARGE STATES OBSERVED IN THE SOLAR WIND

F.M. Ipavich, A.B. Galvin, G. Gloeckler
University of Maryland
Department of Physics and Astronomy
College Park, MD 20742

D. Hovestadt, B. Klecker, M. Scholer
Max-Planck-Institut fur Physik und Astrophysik
Institut fur extraterrestrische Physik
8046 Garching, W. Germany

ABSTRACT

We report solar wind measurements from the ULECA sensor of the Max-Planck-Institut/University of Maryland experiment on ISEE-3. The low energy section of the ULECA sensor selects particles by their energy per charge (over the range ~3.6 keV/Q to ~30 keV/Q) and simultaneously measures their total energy with two low-noise solid state detectors. In this paper we present solar wind Fe charge state measurements from three time periods of high speed solar wind occurring during a post-shock flow and a coronal hole-associated high speed stream. Analysis of the post-shock flow solar wind indicates the charge state distributions for Fe were peaked at ~+16, indicative of an unusually high coronal temperature ($\sim 3 \times 10^6$K). In contrast, the Fe charge state distribution we observe in a coronal hole-associated high speed stream peaks at ~+9, indicating a much lower coronal temperature ($\sim 1.4 \times 10^6$K). This constitutes the first reported measurements of iron charge states in a coronal hole-associated high speed stream.

Introduction

The state of ionization of the solar wind is "frozen in" at low coronal altitudes and remains essentially unchanged during the solar wind's passage through the upper solar atmosphere and interplanetary space (Hundhausen et al., 1968). Measurements of heavy ion (Z>2) charge state abundances in the solar wind are used to estimate the local electron temperature at the coronal freezing-in site. In general, the more massive the element, the higher its freezing-in altitude. For example, interstream solar wind oxygen ions freeze in at ~1.5 solar radii while iron charge states are set at ~3 solar radii (Bame et al., 1974). Measurements of the charge states of different elements can therefore be used to determine temperature gradients in the corona. In addition, the ionization states are indicative of the type of solar wind flow and its origin on the coronal disc. Feldman et al. (1981) have reported moderate ionization temperatures for interstream (IS) solar wind, with average values of $\sim 2.1 \times 10^6$K for oxygen ions and $\sim 1.6 \times 10^6$K for iron ions. They suggest that IS solar wind may originate in near-equatorial coronal streamers, which have similar temperatures. Solar wind post-shock flows (PSFs) and helium abundance enhancements (HAEs) generally have iron and oxygen ionization states indicative of hotter than usual coronal temperatures ($>2.3 \times 10^6$K), with origins in solar active regions (Bame et al., 1979; Fenimore, 1980).

All of the studies cited above use data obtained from solar wind electrostatic analyzer experiments which, for reasons discussed below, have been

unable to resolve heavy ion charge states in coronal hole-associated high speed streams. Using data from the solar wind ion mass-per-charge spectrometer on ISEE-3, Ogilvie and Vogt (1980) have reported oxygen ionization temperatures up to ~3 x 10^6K for high speed solar wind flows which may be coronal hole-associated. Their instrument is limited to speeds below ~600 km/s. Galvin et al. (1982) report much lower ionization temperatures (between ~1.1 x 10^6K and ~1.5 x 10^6K) for coronal hole-associated high speed streams (with speeds ranging from ~500 to ~700 km/s), based on charge state measurements of locally accelerated solar wind heavy ions in diffuse ion events observed upstream of the earth's bow shock. High speed stream Fe/H abundance ratios have been reported by Mitchell and Roelof (1980), but they make no charge state measurements.

The data presented in this paper were obtained with the Ultra Low Energy Charge Analyzer (ULECA) sensor of the Max-Planck-Institut/University of Maryland experiment on ISEE-3. The ULECA sensor is an electrostatic deflection system with an array of solid state detectors. The selection of incoming ions with a given energy per charge window and the measurement of their total energy allow the determination of the charge state distribution. The data presented are from the ULECA L1 and L2 detectors, which respectively cover the energy ranges ~4-11 keV/Q and ~10-30 keV/Q in 32 logarithmic steps with a cycle time of ~16 minutes. The L1 and L2 detectors have energy per charge bandwidths (FWHM/mean) of ~12% and ~21%, respectively, and energy thresholds ~15 keV. We report solar wind measurements from three time periods of high speed solar wind. In particular, we present charge state measurements of iron ions in both a post-shock flow and a coronal hole-associated high speed stream. This is the first reported measurement of iron charge states in a high speed stream.

Observations

The time periods we discuss occurred on Sept. 28 and 29, 1978, during which several distinct types of solar wind flows were observed. During most of Sept. 28, the solar wind may be characterized as a coronal-hole associated high speed stream (Solar-Geophysical Data, 1978). At ~2040 UT on the 28th an interplanetary shock was detected by ISEE-3. At ~0230 UT on the 29th we infer the passage of a much stronger interplanetary shock. Unfortunately, this shock passage occurred during a three hour telemetry gap. Our inference of the presence of this shock is based on a well defined SSC at earth at 0301 UT (Solar-Geophysical Data, 1978) and the detection at ISEE-3 of a classical Energetic Storm Particle event (Klecker et al., 1981; Hovestadt et al., 1982) preceding and following the inferred passage of the interplanetary shock. At ~0815 UT there was a tangential discontinuity in the interplanetary magnetic field and a dramatic decrease in the solar wind ion kinetic temperature. These signatures are often associated with the arrival of flare-generated driver plasma (e.g., Bame et al., 1979). The shock-producing flare was probably a 2B flare (N27, W19) which occurred at 1428 UT on Sept. 27 (Solar-Geophysical Data, 1979), implying an average shock propagation speed of ~1150 km/s.

The sequence of a coronal hole-associated high speed stream followed by two interplanetary shocks led to extremely large solar wind speeds on Sept. 29. Figure 1 shows our observations of proton and helium velocities from 0500 to 1800 UT on Sept. 29. The estimated error in these velocities is ~5%. We point out that solar wind protons are detected by the ULECA sensor only through multiple pulse pile-up; the energy of each of these protons is well below the threshold of the solid state detectors. As a consequence, only a small fraction

(~10^{-3}) of the incident protons is actually counted by the detectors. Although this precludes a computation of the proton density, the peak position in energy per charge (i.e., the voltage step with the highest counting rate) is a reliable measure of the proton velocity. Only protons with velocities above ~800 km/s can pass through the electrostatic deflection analyzer; hence in Figure 1 no proton data are shown after ~1000 UT. Helium ions deposit energies slightly below detector thresholds, but the finite electronic and detector noise produces an efficiency of ~10% (which dominates the effect of helium pile-up). Heavier ions are detected with near unity efficiency. The helium velocities shown in Figure 1 were derived by comparing the observed data with the results of a computer simulation which takes into account all known instrumental effects. The simulation assumes that helium and heavier ions have a common velocity (Schmidt et al., 1980; Ogilvie et al., 1982), and uses the relative elemental abundances presented in Table 1.
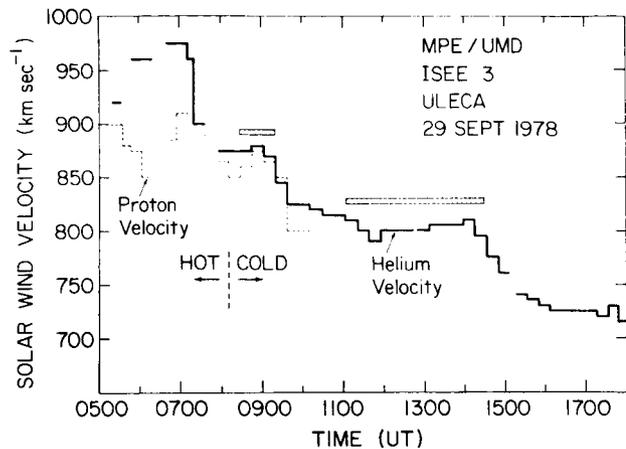
Figure 1. Helium and proton solar wind velocities during the post shock flow on 29 Sept 1978. A large magnetic field tangential discontinuity at ~0815 separates shock-heated solar wind ("HOT") from the flare-associated driver gas ("COLD"). We infer that the interplanetary shock passage occured at ~0230. The hatched bars indicate time periods selected for pulse height analysis.

Table 1

Solar Wind
Adopted Elemental Abundances

Element	Relative Abundance	Reference[*]
H	$\equiv 1 \times 10^6$	a
He	4×10^4	a,b
C	520	d
N	145	c
O	520	a,c,d
Ne	75	b
Mg	75	c
Si	75	a,c
S	26	c
Fe	53	a

[*]
a Solar wind E/Q measurement (Bame et al.,1975)
b Solar wind foil measurement (Geiss,1973)
c Coronal observation (Withbroe,1976)
d Corotating Particle Events (Gloeckler et al.,1979)
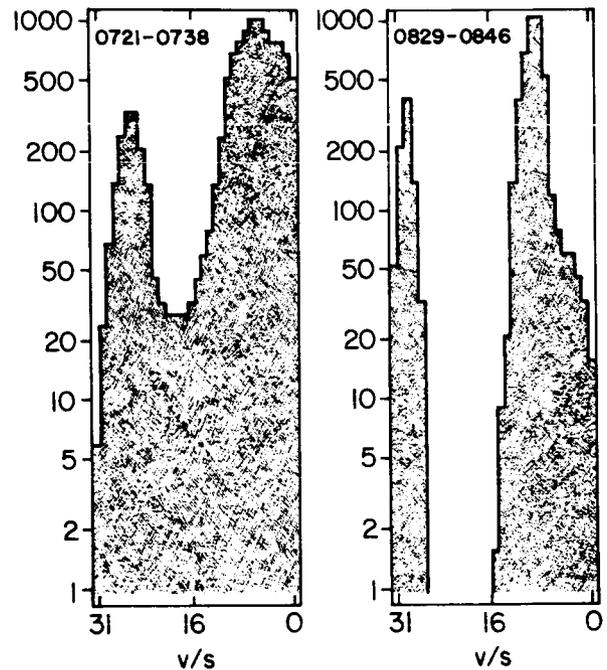
MPE/U of Md.
ULECA
ISEE 3
29 SEPT 1978

Figure 2. Energy per charge spectra for time periods before (left panel) and after (right panel) the passage of the magnetic field tangential discontinuity. Detector L1 counting rates (normalized to 1000 in each panel) are plotted vs. deflection system voltage step (v/s). The 32 logarithmically spaced voltage steps cover the range 3.6 keV/Q (step 31) to 10.6 keV/Q (step 0).

Figure 2 shows energy per charge spectra from detector L1 for time periods before and after the arrival of the driver plasma. The leftmost peak in each panel is due to solar wind protons while the rightmost peak represents helium and heavier ions. The proton counting rate is severely depressed by the detector threshold, as mentioned above. The relative widths of the peaks in the left vs. right panels reflect a decrease in the solar wind kinetic temperature by a factor of ~10 near the time of arrival of the tangential discontinuity in the magnetic field; thus Figure 2 indicates the transition from shock-heated ambient plasma to the flare-associated driver plasma.

We have selected two time intervals (represented by the hatched bars in Figure 1) for detailed pulse height analysis of the driver plasma. Figure 3 shows five energy histograms (counts per keV vs. measured energy in the L2 solid state detector) summed over the time interval 1105-1430 UT. Each of the panels represents a different energy per charge range (i.e., different steps of the electrostatic deflection analyzer). Since solar wind ions moving at the same velocity have kinetic energies proportional to their mass, each energy histogram may be interpreted as a mass histogram. During this time interval we observed a helium velocity of 800 km/s. The vertical dashed lines shown in Figure 3 represent the expected FWHM measured energies for Fe ions at this velocity, based on pre-flight calibrations. There is good agreement with the observed energy histograms for the four lowest panels. The topmost panel (representing the lowest energy per charge range) indicates the presence of an additional ion, consistent with the expected position of Si. Note that by measuring the energy of heavy solar wind ions we can identify their mass directy rather than relying on indirect (albeit convincing) inference based on mass per charge values (e.g., Bame et al., 1979) or assumed (albeit reasonable) solar wind abundance ratios (Mitchell and Roelof, 1980). We point out that the assumed abundances given in Table 1 were used to derive the solar wind He velocity, but not to identify the presence of solar wind Fe.
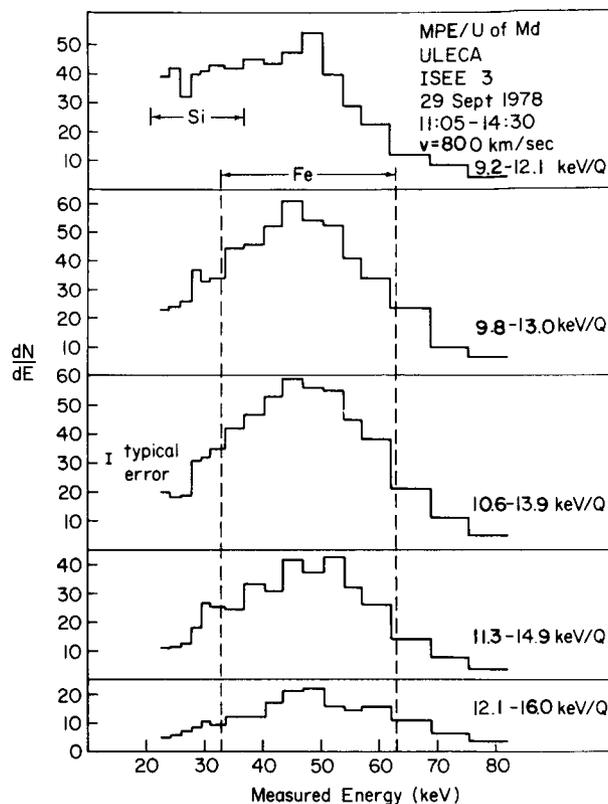

Figure 3. Energy histograms averaged over the time period 1105-1430 UT. Counts per keV is plotted vs. measured energy in the L2 detector. Each panel covers a different energy per charge range. Also indicated are the expected measured energies of Fe and Si ions moving at 800 km/s.

After this identification of Fe based on measured energy, we can convert the fluxes in different energy per charge ranges into a distribution of charge states. We accomplish this by first selecting an energy interval which is high enough to assure no contribution from lighter ions. The number of Fe counts in this interval is then computed for each energy per charge range. This distribution of Fe counts vs. E/Q is then compared with the distribution expected from a simulated solar wind characterized by a particular charge state

freezing-in temperature. A specific temperature corresponds to a unique Fe charge state distribution (we use the density-independent tables of Jordan, 1969). The results of such a comparison for the 1105-1430 time period are presented in Figure 4a. The observations are represented by the solid line while the simulated distributions for two different temperatures are shown as dashed lines. It is clear that the simulation characterized by 3.16 x 10^6K is a much better fit to the observations. Figure 4a also indicates the E/Q positions of Fe charge states 10, 13, and 16. The peak of the observed distributions is seen to be closest to the position expected for Fe^{+16}.

The above analysis was repeated for the time period 0828-0920 (leftmost hatched bar in Figure 1), which is also in the flare-driven piston plasma. The result is shown in Figure 4b. The shift of the Fe charge state positions to higher E/Q values, and the higher energy range over which the Fe pulse height is summed, is caused by the higher solar wind velocity during this time interval. The observed Fe distribution is again fit reasonaby well by a freezing-in temperature of 3.16 x 10^6K.

Our observations thus indicate that the driver plasma was heated to a very high temperature, ~3 x 10^6K, by the solar flare. The simultaneously observed low kinetic temperature then suggests a magnetic topology which restricts heat transport from the corona. Such a scenario has been previously proposed by, e.g., Bame et al. (1979).
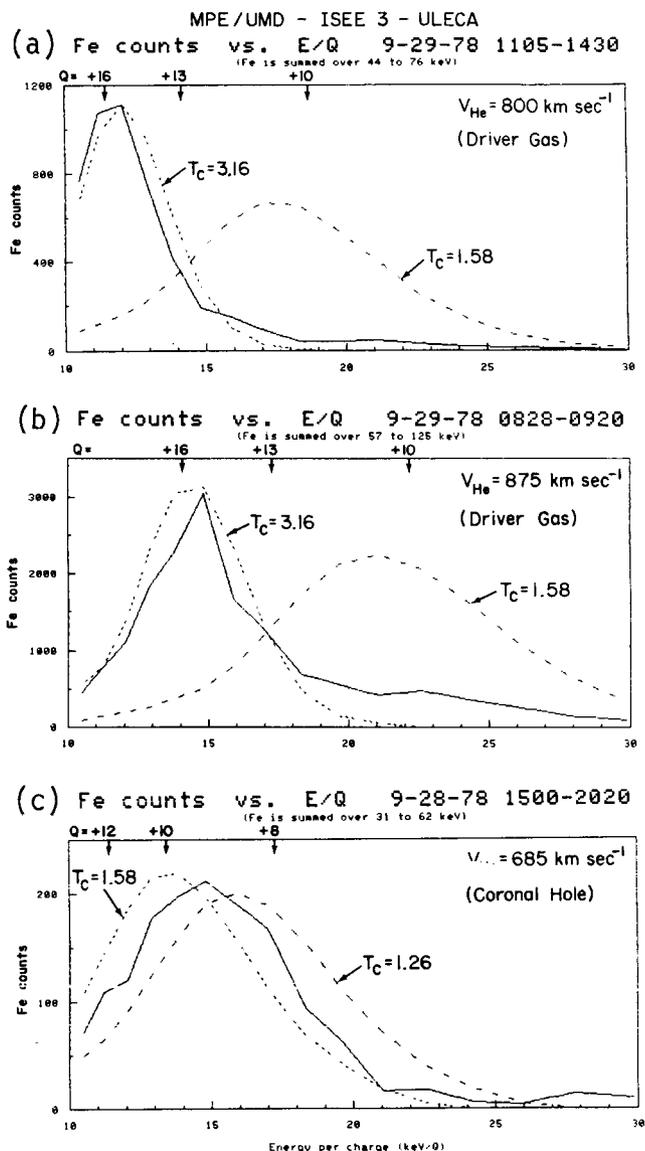

Figure 4. Fe counts vs. energy per charge in the L2 detector for the indicated time periods. The solid lines represent the observations while the dashed lines represent expected distributions for different values of the coronal electron temperature (T_c, in 10^6K) at the freezing-in altitude. The arrows show the positions of different Fe charge states based on the observed solar wind helium velocity.

The final time period we discuss is 1500-2020 UT on 28 Sept. 1978, which is before the arrival of the two interplanetary shocks. As mentioned above, the solar wind during this time period may be characterized as a coronal hole-associated high speed stream. The helium velocity was observed to be reasonably steady, with an average value of 685 km/s. Figure 4c shows the observed distribution of Fe counts vs. energy per charge. Also indicated are the expected distributions corresponding to freezing-in temperatures of 1.26 x 10^6K and 1.58 x 10^6K. We estimate that the observed distribution corresponds to a

temperature of 1.4×10^6 K. The peak of the charge state distribution is near Fe^{+9}. We point out that Figure 4c represents the first observations of Fe charge states in a high speed stream. The reason such measurements have not been previously reported is twofold: a) the high kinetic temperatures in high speed streams make it difficult to identify ions based on energy per charge peaks, and b) the combination of high velocity with low charge states implies heavy ions have very high energy per charge values; thus Figure 4c shows the peak of the Fe charge state distribution occurs at ~14 keV/Q, which is above the range of most solar wind instruments.

Discussion

We have presented measurements of iron charge states in both post-shock flow solar wind and a coronal hole-associated high speed stream. The high ionization temperatures (~3×10^6 K) we obtain for PSF iron are typical of flare-expelled solar wind. Bame et al. (1979), for example, have reported ionization temperatures between ~2.5×10^6 K and ~3.0×10^6 K for PSF iron. Our PSF results support those reported previously and extend them in two respects: (1) Our iron measurements were made at higher solar wind velocities. Whereas we present results at 800 km/s and 875 km/s, iron measurements by the Vela instruments are limited to speeds <650 km/s (Bame et al., 1979; Fenimore, 1980). (2) Bame et al. and Fenimore identify different ion species solely from E/Q spectra, which they convert to M/Q spectra by assuming a common bulk velocity for all heavy ions. Although we also assume all heavy ions flow at about the same speed as helium, our additional measurement of total energy allows the direct determination of the mass of the incoming particles. We can therefore unambiguously distinguish between, e.g., iron and silicon, even when these ions overlap in M/Q spectra.

We also report the first measurement of iron charge states in a coronal hole-associated high speed stream. Such measurements have previously been precluded by the high kinetic temperatures and energy per charge values of these ions in high speed streams. Model calculations based on EUV observations predict that coronal holes are cooler than the average quiet sun and have smaller temperature gradients (Munro and Withbroe, 1972). Estimates for the equilibrium temperatures in coronal holes generally range from ~1×10^6 K to ~1.5×10^6 K (e.g., Kopp and Orrall, 1976; Krieger et al., 1973; Mariska, 1978). These theoretical values are consistent with our measured result of $(1.4 \pm .2) \times 10^6$ K derived from iron charge states.

In contrast, Ogilvie and Vogt (1980), using data from an ion mass-per-charge spectrometer, find that the ionization temperature for oxygen ions in the solar wind rises rapidy with speed, reaching more than 3×10^6 K for speeds ~600 km/s. They suggest the apparent discrepancy with theoretical expectations may be the result of non-Maxwellian electron velocity distributions in the corona where freezing-in occurs. Indeed, Owocki (1982) predicts that ionization temperatures inferred from O^{+6}/O^{+7} ratios in the solar wind could overestimate the actual coronal electron temperatures if the assumption of a Maxwellian distribution was incorrect. However, he estimates the magnitude of the possible temperature overestimate is limited to ~0.8×10^6 K, only partially explaining the above-mentioned discrepancy. Although our results indicate a much lower temperature than the Ogilvie and Vogt data, it should be noted that we are observing a different ion species (iron instead of oxygen) at a somewhat higher velocity (685 km/s instead of 600 km/s).

Galvin et al. (1982) report ionization temperatures between ~1.1 x 10^6K and ~1.5 x 10^6K for coronal hole-associated high speed streams, based on the charge state analysis of energetic upstream diffuse ions (which are presumed to be solar wind ions accelerated by the earth's bow shock) observed during high speed streams. Although their analysis technique requires certain assumptions, their derived temperatures are very different from those of Ogilvie and Vogt but are consistent with our measurements for iron. In addition, Galvin et al. find that the coronal hole-associated ionization temperatures are approximately constant over the range of solar wind speeds covered (~500-700 km/s), a result which also differs from that of Ogilvie and Vogt. The Galvin et al. results are derived from the overall charge state distribution of Z>2 ions, in contrast to the O^{+6}/O^{+7} ratio determination by Ogilvie and Vogt. However, because oxygen and carbon dominate the other heavy ions in the solar wind (see Table 1) the results should be comparable, unless carbon ions behave in some very unexpected manner. In this context we note that C^{+6}, expected to be the most abundant heavy ion in the solar wind, has never been identified because its mass per charge value is identical to that of the much more abundant He^{+2}.

Our present results for high speed stream iron indicate low ionization temperatures are present in coronal holes where freezing-in occurs. In addition, these results combined with those of Galvin et al. for carbon and oxygen would imply: (a) there are at most modest deviations from Maxwellian conditions in coronal holes, and (b) the electron temperature gradient over the range of freezing-in altitudes is quite small in coronal holes.

References

Bame, S.J., J.R. Asbridge,W.C. Feldman and P.D. Kearney, The quiet corona: temperature and temperature gradient, Solar Physics, 35, 137, 1974.

Bame, S.J., J.R. Asbridge, W.C. Feldman, M.D. Montgomery and P.D. Kearney, Solar wind heavy ion abundances, Solar Physics, 43, 463, 1975.

Bame, S.J., J.R. Asbridge, W.C. Feldman, E.E. Fenimore and J.T. Gosling, Solar wind heavy ions from flare-heated coronal plasma, Solar Physics, 62, 179, 1979.

Feldman, W.C., J.R. Asbridge, S.J. Bame, E.E. Fenimore and J.T. Gosling, The solar origins of solar wind interstream flows: near-equatorial coronal streamers, J. Geophys. Res., 86, 5408, 1981.

Fenimore, E.E., Solar wind flows associated with hot heavy ions, Astrophys. J., 235, 245, 1980.

Galvin, A.B., F.M. Ipavich and G. Gloeckler, Solar wind ionization temperatures inferred from the charge state analysis of diffuse ion events (abstract), EOS Trans. AGU , 63, 424, 1982.

Geiss, J., Solar wind composition and implications about the history of the solar system, Proc. 13th Intl. Cosmic Ray Conf., 5, 3375, 1973.

Gloeckler, G., D. Hovestadt and L.A. Fisk, Observed distribution functions of H, He, C, O and Fe in corotating energetic particle streams: implications for interplanetary acceleration and propagations, Astrophys. J., 230, L191, 1979.

Hovestadt, D., B. Klecker, H. Hofner, M. Scholer, G. Gloeckler and F.M. Ipavich, Ionic charge state distribution of He, C, O and Fe in an energetic storm particle enhancement, Astrophys. J. Lett., 258, L57, 1982.

Hundhausen, A.J., H.E. Gilbert and S.J. Bame, Ionization state of the interplanetary plasma, J. Geophys. Res., 73, 5485, 1968.

Jordan, C., The ionization equilibrium of elements between carbon and nickel, Mon. Not. R. Astr. Soc., 142, 501, 1969.

Klecker, B., M. Scholer, D. Hovestadt, G. Gloeckler and F.M. Ipavich, Spectral and compositional variations of low energy ions during an energetic storm particle event, Astrophys. J., 251, 393, 1981.

Kopp, R.A. and F.Q. Orrall, Temperature and density structure of the corona and inner solar wind, Astron. Astrophys., 53, 363, 1976.

Krieger, A.S., A.F. Timothy and E.C. Roelof, A coronal hole and its identification as the source of a high velocity solar wind stream, Solar Physics, 29, 505, 1973.

Mariska, J.T., Analysis of extreme-ultraviolet observations of a polar coronal hole, Astrophys. J., 225, 252, 1978.

Mitchell, D.G. and E.C. Roelof, Thermal iron ions in high speed solar wind streams: detection by the IMP 7/8 energetic particle experiments, Geophys. Res. Lett., 7, 661, 1980.

Munro, R.H. and G.L. Withbroe, Properties of a coronal "hole" derived from extreme-ultraviolet observations, Astrophys. J., 176, 511, 1972.

Ogilvie, K.W. and C. Vogt, Variation of the average 'freezing-in' temperature of oxygen ions with solar wind speed, Geophys. Res. Lett., 7, 577, 1980.

Ogilvie, K.W., M.A. Coplan and R.D. Zwickl, Helium, hydrogen, and oxygen velocities observed on ISEE-3, J. Geophys. Res., 87, 7363, 1982.

Owocki, S.P., Interpreting the solar wind ionization state, Solar Wind 5, Woodstock, Vt., (these Proceedings), 1982.

Schmidt, W.K.H., H. Rosenbauer, E.G. Shelley and J. Geiss, On temperature and speed of He^{++} and O^{6+} ions in the solar wind, Geophys. Res. Lett., 7, 697, 1980.

Solar-Geophysical Data, 411 Part I, U.S. Department of Commerce, Boulder, Colorado, 1978.

Solar-Geophysical Data, 415 Part II, U.S. Department of Commerce, Boulder, Colorado, 1979.

Withbroe, G.L., The chemical composition of the photosphere and corona, Harvard College Observatory Preprint Series No. 524, 1976.